



## Method for modifying the morphology of silica particles derived from sodium metasilicate

Enobong R.Essien<sup>1\*</sup>, Oluyemi Olaniyi<sup>1</sup>, Luqman A.Adams<sup>2</sup>, Rafiu O.Shaibu<sup>2</sup>, Tony Chukwu<sup>2</sup>

<sup>1</sup>Department of Chemical Sciences, Bells University of Technology, P.M.B. 1015, Ota, Ogun State, (NIGERIA)

<sup>2</sup>Department of Chemistry, Faculty of Science, University of Lagos, (NIGERIA)

E-mail : reggiessien@gmail.com

### ABSTRACT

Particle size, pore size, surface area as well as the morphology of silica particles prepared from sodium metasilicate have been modified using two acid catalysts. Gel formation was obtained at ambient conditions using HCl and H<sub>2</sub>SO<sub>4</sub>. The obtained particles were characterized using scanning electron microscopy (SEM), X-ray diffraction (XRD), Fourier transform infrared spectroscopy (FTIR) and mathematical techniques. The results showed amorphous silica particles were successfully formed. XRD investigation revealed that the materials contained amorphous SiO<sub>2</sub>, while SEM results indicated that different porous morphologies were obtained from the two different acid catalysts.

© 2014 Trade Science Inc. - INDIA

### KEYWORDS

Silica particles;  
Sodium metasilicate;  
Amorphous SiO<sub>2</sub>.

### INTRODUCTION

Porous silica is widely used in catalysis, purification<sup>[1,2]</sup> and chemical sensors<sup>[3]</sup> because it is characterized by large surface area, high mechanical strength and thermal resistance. There has been increasing efforts aimed at improving the morphological characteristics, such as particle sizes, and pore structure of silica as a way of improving mass transfer efficiency. According to studies<sup>[4]</sup>, the connectivity of the pore structure as well as permeability of the porous network can be controlled and modelled. In this regard, the nature of acid or base catalyst, pH of the solution, the solvent, the temperature and relative humidity are all crucial in controlling porosity<sup>[5]</sup>.

The most general method of synthesizing microporous silica usually involves using templates such as carbon nanotubes<sup>[6]</sup>, porous alumina<sup>[7]</sup>, organic gels<sup>[8]</sup>, organic crystals<sup>[9]</sup> and surfactants<sup>[10,11]</sup>. These templates are commonly used with silica precursors such as alkyl alkoxides which facilitates covalent bonding and can then be removed by calcinations thereby leading to the creation of a continuous network of microspores. However, the relatively high cost of silicon alkoxide precursors and templates, and the difficulty in completely removing the templates from the prepared porous materials limit their usage.

In the current work, we employed two acid catalysts (HCl and H<sub>2</sub>SO<sub>4</sub>) to tune the morphology of silica prepared from sodium metasilicate.

## Full Paper

### MATERIALS AND METHODS

#### Materials

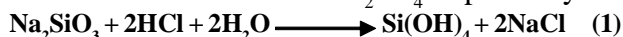
The chemicals used in this synthesis were sodium metasilicate,  $\text{Na}_2\text{SiO}_3$  with composition  $\text{SiO}_2$  24.9,  $\text{Na}_2\text{O}$  20.9 and  $\text{H}_2\text{O}$  54.2 wt % (Sigma-Aldrich, 98%),  $\text{H}_2\text{SO}_4$  (Analar, 98%) and HCl (Riedel-deHaen, 37%).

#### Preparation of porous silica particles using HCl (HCPSP) and $\text{H}_2\text{SO}_4$ (HSPSP)

$\text{Na}_2\text{SiO}_3$  (5.0 g) was dissolved in deionised water (10.0 ml) while stirring using a magnetic stirrer. Thereafter 2M HCl (20.0 ml) was added dropwise until a gel was formed at room temperature after about 5 minutes of stirring. The experiment was repeated using 2M  $\text{H}_2\text{SO}_4$  (10.0 ml) under similar reaction conditions.

#### Washing procedures

The gel formed was washed by pouring into deionized water (100 ml x 5), the supernatant water was decanted successively<sup>[12]</sup> to remove impurities of NaCl and  $\text{Na}_2\text{SO}_4$  formed during the hydrolysis stage of the reaction, equations (1) and (2), before drying by suction at the pump. Complete removal of impurities from the gel network was confirmed by absence of precipitate when the final filtrate was tested variously with dilute  $\text{AgNO}_3$  and lead (II) ethanoate solutions to confirm absence of NaCl and  $\text{Na}_2\text{SO}_4$  respectively.



#### Thermal treatment

The washed gels were initially dried at 120 °C for 1 day, and then calcined at 800 °C for 3 hours in a furnace with a heating rate of 10 °C/min. The irregular powder obtained were ground by ball-milling.

#### Methods of characterization

The silica particles was characterized by X-ray diffraction (XRD, X'pert PRO PANalytical) using  $\text{CuK}\alpha$  radiation (0.154060) source operated at 40 kV and 40 mA. The diffraction patterns were obtained in the  $2\theta$  range from 5-120° and 10-70°. The morphologies of the materials were investigated using scanning electron microscopy (SEM, EVO/MAIO). SEM was also used to determine the average size of the silica particles. The sample was carbon-coated and

observed at an accelerating voltage of 10 kV. Fourier transform infrared (FTIR, Buck Scientific 500), in the wavenumber range of 4000-600  $\text{cm}^{-1}$  employing KBr pellets was used to investigate the bonds present in the particles.

The bulk densities of the silica particles were measured from their weight to volume ratio using the formula

$$\text{Bulk density, } \gamma_b = M / V \quad (3)$$

where, M is the mass of the sample measured with microbalance (10<sup>-5</sup> g accuracy), and V is the volume measured by filling the silica particles in a column of known volume<sup>[13]</sup>.

The specific surface area of the particles in  $\text{m}^2\text{g}^{-1}$  was calculated using the equation<sup>[14,15]</sup>

$$\text{Specific surface area, } S_p = 6 / \Gamma_p D_p \quad (4)$$

in which  $\Gamma_p$  is specific density assumed to be 2.0 x 10<sup>6</sup>  $\text{gm}^{-3}$  for amorphous silica particles based on the spherical model (a typical average density of silica prepared via wet-synthesis conditions<sup>[16]</sup>) and  $D_p$  is the average particle diameter.

The porosity was estimated using the relationship<sup>[17]</sup>.

$$\text{Porosity} = (1 - \gamma_b / \Gamma_p) \times 100 \quad (5)$$

## RESULTS AND DISCUSSION

### Hydrolysis, gelation, gel washing and calcination

The sodium metasilicate used here as cheap silica precursor was easily hydrolyzed by both acids to give a transparent gel at ambient temperature. The gels were washed in deionised water to remove sodium sulphate and sodium chloride salts. The dried gel were then calcined followed by ball milling to give the porous silica powders.

### Diffraction Patterns of the porous silica particles

The XRD patterns of the HCPSP and HSPSP powders obtained after calcination at 800 °C are shown in Figure 1(a) and (b) respectively. The diffraction patterns of the samples with a reflection at  $2\theta = 22-22.5^\circ$  indicate that the materials are amorphous and composed of  $\text{SiO}_2$ <sup>[18-20]</sup>. There are no additional peaks observed in both spectra which indicate the absence of impurities after deionised water washing removal of NaCl and  $\text{Na}_2\text{SO}_4$  from the gel networks.

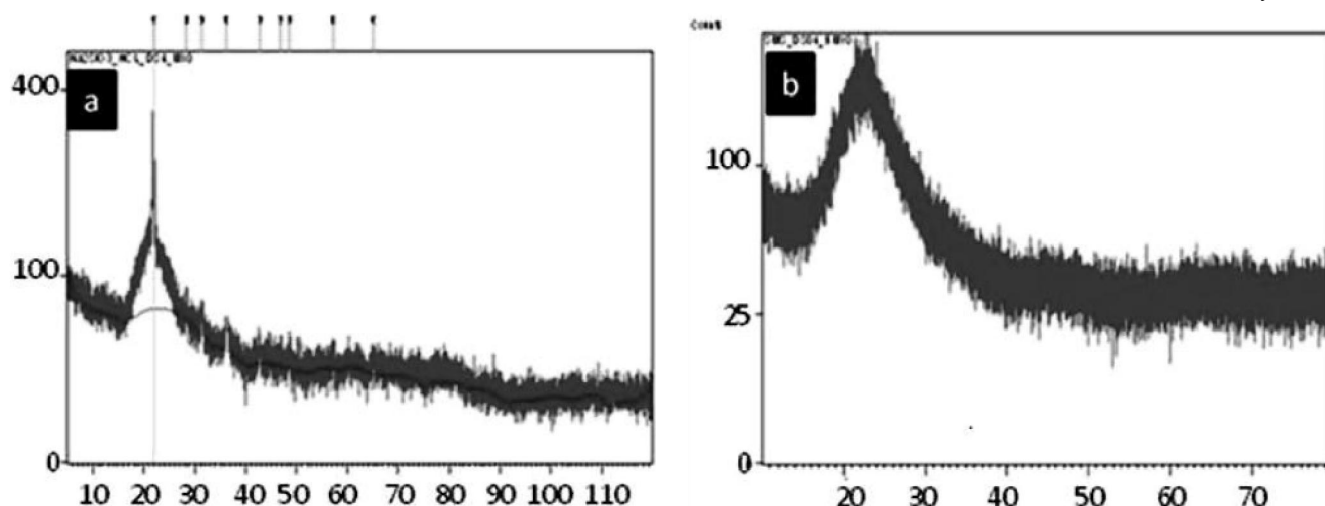


Figure 1 : XRD patterns of calcined samples of (a) HCPSP and (b) HSPSP powders at 800 °C

### Assessment of bonding in the particles

FTIR spectrum of HCPSP powders is shown in Figure 2. The characteristic vibrational modes of Si–O–Si bonds are distinctive around 804.38  $\text{cm}^{-1}$  and 1071.43  $\text{cm}^{-1}$ , which are attributed to Si–O bending vibration and Si–O–Si asymmetric stretching vibration respectively<sup>[21,22]</sup>. The band at 1656.22  $\text{cm}^{-1}$  is assigned to Si–H<sub>2</sub>O flexion<sup>[22]</sup>. It is noted that the Si–O–Si asymmetric stretching band for HSPSP, Figure 3, occurs at 1066.52  $\text{cm}^{-1}$  which is lower than that of HCPSP. This supports Labrosse *et al.*'s<sup>[23]</sup> report that a shift in vibrational frequency is related to porosity. It is also observed that a typical broad absorption band between 3000–3586.24  $\text{cm}^{-1}$  centred at 3506.40  $\text{cm}^{-1}$  which can be attributed to adsorbed water or structural O–H<sup>[24]</sup> are less intense in the spectra of both HCPSP and HSPSP.

This is mainly due to the removal of most of the adsorbed water molecules during the calcination process up to 800 °C. This can be confirmed by the diffuse nature of the peak around 1656.22  $\text{cm}^{-1}$  in the two spectra which is usually prominent in wet sol-gel-derived silica as a result of Si–H<sub>2</sub>O flexion<sup>[21]</sup>.

### Morphology of the porous silica particles

The average diameter of the silica particles as determined by SEM gave the average particle diameter for the HCPSP as 597.95 nm, while the average diameter of the HSPSP was 373.75 nm. Figure 4 presents the morphology of silica particles calcined at 800 °C. The result shows that the particles are arranged to give porous network structure. Discrete particles and some few agglomerates are seen in the micrographs of both samples, especially that of HCPSP sample. This mor-

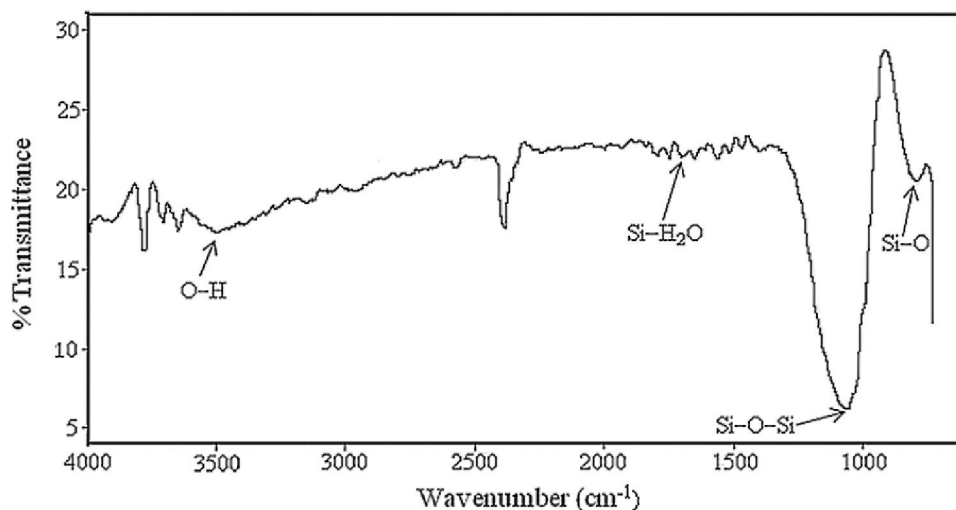


Figure 2 : FTIR spectrum of HCPSP after calcination at 800 °C.

## Full Paper

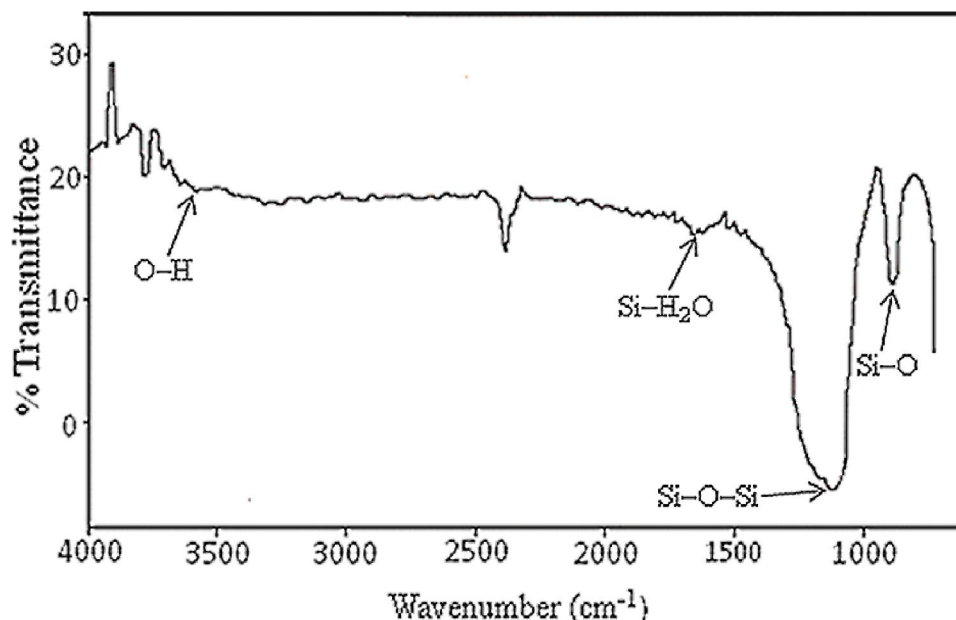


Figure 3 : FTIR spectrum of HSPSP after calcination at 800 °C.

phological transformation occurs as a result of sintering, which according to Moya *et al.*<sup>[25]</sup>, is driven by the tendency to reduce the total free energy by reducing the total surface thus causing the adhering and aggregation of particles. Another important process effective at high temperatures below the melting point is viscous flow which can result in neck formation and densification and further restructuring<sup>[26]</sup>.

It is observed that the silica networks contain particles and pore sizes that are not uniform. This may be attributed to agglomeration usually associated with silica particles obtained from sodium metasilicate solution<sup>[27]</sup>. Agglomeration was higher in the HCPSP sample, Figure 4(a), which consequently has larger particle sizes

and average pore size ranging from 0.18 - 0.91  $\mu\text{m}$ , while the HSPSP sample with smaller particles has pore sizes ranging from 0.10-0.40  $\mu\text{m}$ . According to Dafni *et al.*<sup>[28]</sup>, the porosity arises from the assumed packing of primary particles in the agglomerates. It has been proposed that the initial particle size distribution, polydispersity, concentration of particles, viscosity of the continuous phase, Van der Waals forces of attraction, and hydrodynamic conditions govern the extent of interparticle collisions, aggregation and the temporal evolution of the average diameter of aggregates<sup>[29]</sup>. In this regard, we suggest that apart from the foregoing factors, the nature and concentration of the salt formed ( $\text{NaCl}$  and  $\text{Na}_2\text{SO}_4$ ) during the gelation process of the

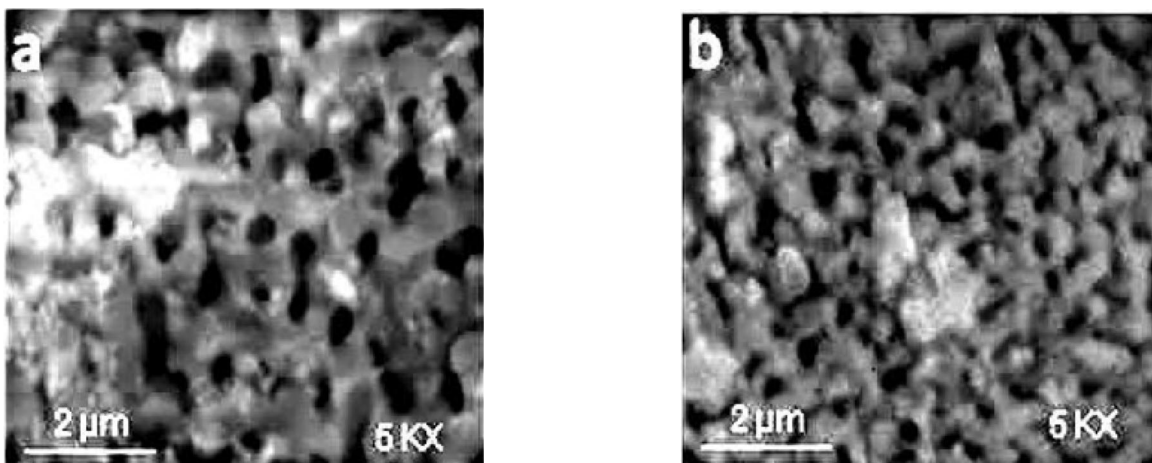


Figure 4 : SEM micrographs showing larger pore spaces in (a) HCPSP, than (b) HSPSP at the same magnification.



reaction contributed to the observed size of the particles and pores to complement Božena *et al.*'s<sup>[27]</sup> suggestion that electrolytes also affect the physiochemical properties of silica.

### Physiochemical properties of HCPSP and HSPSP

The physicochemical properties of the obtained silicas are listed in TABLE 1. The surface area is highly dependent on average particle size and porosity. HCPSP

have larger average particle size and porosity but smaller surface area, as expected when compared with HSPSP which have lower average particle size and consequently larger surface area. This order is in agreement with the SEM results. A sensible correlation between porosity and Si–O–Si absorption frequency could be made from the result in TABLE 1. It is observed that the higher the porosity, the higher the absorption frequency of the Si–O–Si bonds in the particles.

TABLE 1 : Physiochemical properties of the silica particles and Si-O-Si absorption frequency

Sol-gel derived silica	Average particle diameter (nm)	Bulk density (Mgm <sup>-3</sup> )	Pore size range (µm)	Porosity (%)	Specific surface area, S <sub>T</sub> (m <sup>2</sup> g <sup>-1</sup> )	Frequency of Si–O–Si bond (cm <sup>-1</sup> )
HCPSP	597.95	0.474	0.18-0.91	76.3	5.017	1071.43
HSPSP	353.75	0.752	0.10-0.40	62.0	8.58	1066.52

### CONCLUSIONS

HCl and H<sub>2</sub>SO<sub>4</sub> have been successfully used to tune the pore structures and particle sizes of silica particles obtained from sodium silicate as a cheap silica source without employing templates. When HCl was used to catalyze gelation, the average particle size obtained was 597.95 nm with pore sizes ranging from 0.18 - 0.91 µm, while for H<sub>2</sub>SO<sub>4</sub> catalyzed gelation a much lower average particle size of 353.75 nm and pore size range of 0.10-0.40 µm was obtained. The relationship between porosity and Si–O–Si vibrational frequency was also established. The results indicate that the morphology of silica particles can be modified by using different types of catalysts and this may provide a useful route for preparing silica with controlled pore sizes without using templates.

### ACKNOWLEDGEMENT

Most part of this work was conducted in Bells University of Technology, Ota, Nigeria. The authors are therefore grateful to the staff of the Central Research Laboratory, Bells University of Technology, Ota for providing their facilities and other necessary assistance for carrying out this project.

### REFERENCES

[1] A.Corma; Chem.Rev., **97**, 2375 (1997).

- [2] K.W.Gallis, J.T.Araujo, K.J.Duff, J.G.Moore, C.C.Landry; Adv.Mater., **11**, 1452 (1999).
- [3] Y.Xi, Z.Liangying, W.Sasa; Sensors and Actuators B, **24,25**, 347 (1995).
- [4] W.I.Vasconcelos; Quim.Nova., **21**, 514 (1998).
- [5] Y.Murakami, K.Tanaka, Y.Takechi, S.Takahashi, Y.Nakano, T.Matsumota, J.Sol-Gel Sci.Technol., **29**, 19 (2004).
- [6] B.C.Satishkumar, A.Gocindaraj, E.M.Vogl, L.Basumallick, C.N.R.Rao; J.Mater.Res., **12**, 604 (1997).
- [7] B.B.Lakshmi, P.K.Dorhout, C.R.Martin; Chem.Mater., **9**, 857 (1997).
- [8] J.H.Jung, Y.Ono, S.Shinkai; Langmuir, **16**, 1643 (2000).
- [9] F.Miyaji, S.A.Davis, J.P.H.Charmant, S.Mann; Chem.Mater., **11**, 3021 (1999)
- [10] M.Adachi, T.Harada, M.Harada; Langmuir, **16**, 2376 (2000).
- [11] A.J.Zarur, N.Z.Mehenti, A.T.Heibel, J.Y.Ying; Langmuir, **16**, 9168 (2000).
- [12] U.K.Bangi, A.V.Rao, A.P.Rao; Sci.Technol.Adv.Mater., **9**, 1 (2008).
- [13] M.S.Poonam, A.V.Rao, A.P.Rao, S.D.Bhagat; J.Sol-Gel Sci.Technol., **49**, 285 (2009).
- [14] S.J.Gregg, K.S.W.Sing; Adsorption, Surface Area and Porosity, 2<sup>nd</sup> Edition, Academic Press: London, (1982).
- [15] E.F.Vansant, P.Van der Voort, K.C.Vrancken; Characterization and Chemical Modification of Silica Surface, 1<sup>st</sup> Edition, Elsevier Science; New York, (1995).
- [16] G.Michael, H.Ferch' Schriftenreihe Pigmente, Degussa, **11**, (1991).

## Full Paper

---

- [17] H.Hunger, H.J.H.Brouwers; Cement and Concrete Comp., **31**, 39 (2009).
- [18] C.Bhavornthanayod, P.Rungrojchaiporn; J.Metals, Materials and Minerals, **19**, 79 (2009).
- [19] P.Sooksaen, S.Suttiruengwong, K.Oniem, K.Ngamlamiad, J.Atireklapwarodom; J.Metals, Materials and Minerals, **18**, 85 (2008).
- [20] U.Kalapathy, A.Proctor, J.Shultz; Bioresour.Technol., **72**, 99 (2000).
- [21] V.El-Rassy, A.C.Pierre; J.Non-Cryst.Solids, **351**, 603 (2005).
- [22] P.Innocenzi, P.Falcaro, D.Grosso, F.Babonneau; J.Phys.Chem.B, **107**, 4711 (2003).
- [23] A.Labrosse, A.Burneau; J.Non-Cryst.Solids, **221**, 107 (1997).
- [24] J.Y.Ying, J.B.Benziger; J.Am.Ceram.Soc., **76**, 2571 (1993).
- [25] J.Moya, C.Baudin, P.Miranzo; In Encyclopedia of Physical Sciences and Technology; R.Meyer, (Eds); Academic Press: San Diego, **15**, (1992).
- [26] T.Poppe; Icarus, **164**, 139 (2003).
- [27] B.Rager, A.Krysztafkiewicz; Colloids Surf.A Physicochem.Eng.Asp., **125**, 121 (1997).
- [28] D.G.Bika, M.Gentzler, J.N.Michaels; Powder Technol., **117**, 98 (2001).
- [29] S.A.K.Jeelani, G.Benoist, K.S.Joshi, R.Gunde, D.Kellenberger, E.J.Windhab; Colloids Surf.A: Physicochem.Eng.Aspects, **263**, 379 (2005).